

Influence of Air-Gap Length on CO₂ Stripping from Diethanolamine Solution and Water Performance of Surface Modified PVDF Hollow Fiber Membrane Contactor

Rahbari-Sisakht, Masoud*⁺; Emadzadeh, Daryoush

Department of Chemical Engineering, Gachsaran Branch, Islamic Azad University, Gachsaran, I.R. IRAN

Fauzi Ismail, Ahmad; Korminouri, Fatemeh; Matsuura, Takeshi*

Advanced Membrane Technology Research Center (AMTEC), Universiti Teknologi Malaysia (UTM),
81310 Skudai, Johor, MALAYSIA

Mayahi, Alireza

Australian Institute for Bioengineering and Nanotechnology (AIBN), University of Queensland,
Brisbane 4072, QLD, AUSTRALIA

ABSTRACT: Surface Modifying Macromolecule (SMM) blended PVDF hollow fibers (HFs) were spun at different air-gaps (0 to 20 cm) and used for CO₂ stripping from aqueous DEA solution and water. The manufactured fibers were firstly subjected to various characterization tests such as contact angle and critical water entry pressure measurement to evaluate the HF hydrophobicity and wetting resistance, respectively. The pure helium permeation experiments were also conducted to obtain membrane pore size and effective porosity. Morphology of the HFs was investigated by Scanning Electron Microscopy (SEM) and Atomic Force Microscopy (AFM). The SEM images showed that both outer and inner diameters of HFs decreased significantly by increasing air-gap length which mainly because of elongation of HF caused by gravity while travelling through the air-gap. Also, the gradual decrease in roughness on the external surface of the produced HFs was observed from the AFM images. It was found that the increase of liquid velocity enhances the CO₂ stripping flux. It was found that 10 cm air-gap gave maximum stripping flux of 3.34×10^{-2} and 1.34×10^{-3} (mol/m² s) for DEA solution and water, respectively. The increase in gas velocity, on the other hand, did not affect the stripping flux significantly. It was observed that the increase of temperature from 25 to 80 °C led to the marked enhancement of stripping flux from 6.30×10^{-3} to 3.34×10^{-2} (mol/m² s) and 6.5×10^{-5} to 1.34×10^{-3} (mol/m² s), for DEA solution and water, respectively. Furthermore, the increase in DEA concentration from 0.25 to 1 mol/L, led to the enhancement of the stripping flux from 6.84×10^{-3} to 3.34×10^{-2} (mol/m² s) at a liquid velocity of 0.7 m/s. It was concluded that the HF spun at 10 cm air-gap exhibited the best stripping performance among all fabricated HFs.

KEYWORDS: PVDF hollow fiber; CO₂ stripping; Membrane contactor; Air-gap length.

* To whom correspondence should be addressed.

+ E-mail: rahbari@iaug.ac.ir ; rahbarisisakht@gmail.com

Other Address: Department of Chemical and Biological Engineering, University of Ottawa, Ontario K1N 6N5, CANADA
1021-9986/2018/4/117-129 13/\$/6.03

INTRODUCTION

Climate change is mostly driven by increasing carbon dioxide (CO₂) levels in the atmosphere, which is the inevitable result of the dependence of industrial and domestic activities on fossil fuels. Although the high degree of dependence on fossil fuels should be eliminated or reduced extensively by using substitute candidates such as nuclear and renewable energy, these resources cannot be used in widespread applications due to their inherent drawbacks. Currently, various technologies based on physical or chemical methods are applied to restrict CO₂ release to the environment. Among these methods, membrane technology has been extensively applied in a variety of fields including gas separation, micro extraction, solvent extraction and etc. In particular, Hollow Fiber Membrane (HFM) contactors are considered as a novel, alternative method for CO₂ removal to replace the conventional technologies by overcoming their shortcomings [1-13]. HFMs offer great potential for both CO₂ absorption and stripping of gas flows. Hence, it is no wonder that a large number of researches have focused on the gas-liquid HFM contactor recently since HFM surpasses excellently the drawbacks of traditional technologies.

One of the noteworthy advantages of HFM based Membrane Contactor (MC) is that it provides a large contact area between the gas and liquid sides without gas and solvent flow mixing. In addition, HFMs can scale up easily, exhibit higher mass transfer rates per unit volume, more compactness, modularity, and flexibility. Additionally, the HFM based MC exhibits the excellent performance for desorption and regeneration of the liquid absorbents. In the absorption procedure, unwanted gas (CO₂) absorbed by the liquid absorbent. In the stripping process desorption of CO₂ takes place from the liquid absorbent at one end of the HFM pore and diffuses through the pore, then is carried away by N₂ (the sweep gas) at the other end of the pore.

The stripping unit is the principally responsible for energy costs in the gas separation processes [14]. The membrane material used for both absorption and stripping should resist wetting and possess high gas permeability, great chemical, and heat-aging endurance. Fabrication of hydrophobic membranes to restrict the wettability is the prominent objective in membrane contactor application, since; wettability of membrane causes the reduction in mass transfer rate and CO₂ flux.

One outstanding method to elevate the hydrophobicity of HFMs is the modification of membrane surface using Surface Modified Macromolecules (SMMs). SMMs are amphiphatic macromolecules composed of hydrophilic and hydrophobic segments, which preferentially migrate to the membrane surface. The SMM structure and the mechanism of its surface migration were previously set out in meticulous details [15]. It is predicted that the air-gap between spinneret and coagulation medium can provide time for SMM to migrate to the HFM surface.

There are a number of works conducted recently to investigate the influence of air-gap on membrane performance [16-22]. Moreover, researches have also been done on CO₂ stripping using various polymeric membranes fabricated under different conditions. For example, research was carried out for CO₂ stripping from aqueous monoethanolamine (MEA) solution employing polytetrafluoroethylene (PTFE) membrane [3]. It was reported that the CO₂ desorption flux enhanced in a higher concentration of MEA. *Naim et al.* [23] produced PVDF membranes using different additives such as, glycerol, methanol, lithium chloride, polyethylene glycol (PEG-400) and phosphoric acid to strip CO₂ from diethanolamine (DEA) solution. Their results showed that PVDF/PEG-400 membrane achieved the maximum stripping flux of 4.03×10^{-2} mol/m².s that can be attributed to the marked gas permeation and noticeable effective surface porosity of the fabricated membrane.

In another work [24], PVDF fibers were developed to investigate the influence of different lithium chloride (LiCl) levels in the casting dope on CO₂ stripping efficiency from aqueous DEA solution. It was found that stripping flux increased with increasing LiCl concentration in the casting solution and the maximum CO₂ flux was achieved at 5 wt.% LiCl.

Hosseini and Mansourizadeh [25] carried out experiments for CO₂ stripping using porous hydrophobic poly(vinylidene fluoride-co-hexafluoropropylene) (PVDF-HFP) fibers spun via wet spinning process while employing DEA solution as the liquid absorbent. The improved PVDF-HFP/PA membrane showed CO₂ stripping flux of about 9×10^{-3} (mol/m² s) at the liquid velocity of 0.045 m/s.

In our previous work [26] surface modified PVDF membranes using SMM were fabricated to strip CO₂ from

aqueous DEA solution. It was found that the increase in DEA concentration or temperature from 80 to 90 °C resulted in the enhancement of CO₂ desorption flux.

To the best of our knowledge, no research has been conducted on the fabrication of PVDF hollow fiber membrane with surface modification by SMM under different air-gap length for CO₂ stripping. Therefore, the aim of the present work is to investigate the influence of SMM migration to the HF surface on the membrane stripping of CO₂ from water and aqueous DEA solution. For this purpose, SMM blended PVDF hollow fibers were spun with different air-gap distances and the membrane so fabricated were further characterized by various methods and subjected to membrane stripping experiments.

EXPERIMENTAL SECTION

Fabrication of PVDF membranes

The PVDF membranes were fabricated from a spinning dope containing 18 wt% PVDF (Kynar grade 740, supplied by Arkema Inc., Philadelphia) and 1 wt% SMM (additive) in N-methyl-2-pyrrolidone as a solvent. The mixture was stirred at 60 °C until homogenous and stable solution was formed. After the casting dope was degassed, the spinning dope were passed through a spinneret and traveled through the air-gap, before being solidified after in the coagulation bath. The air gap was changed from 0 to 20 cm while other spinning conditions remained the same. HFs (M₁-M₅) were spun with different air-gaps of in a laboratory scale. The precise details of HF spinning were given in other literature [27]. The HFs were then stored in tap water to remove the residual solvent for 72 h and subsequently dried at 25 °C before being subjected to further experiments. The HF spinning conditions are tabulated in Table 1.

Morphology of fabricated membranes

In order to study the morphology of fabricated hollow fiber membranes, the images of the cross-section and the outer surface of the hollow fibers were obtained at different magnifications by Scanning Electron Microscopy (SEM) using Tabletop microscope, TM3000, HITACHI. To have a clean break, the hollow fibers were immersed in liquid nitrogen, and then they were dried and coated with sputtering platinum.

Surface morphology analysis

Atomic force microscopy (AFM) was employed to study the morphology of the outer surface of prepared HFs. The images were obtained over a scan area of 4 μm × 4 μm, using AFM device (SPA 300HV, Japan). Detailed descriptions of the method used to take the AFM images were described in other studies [28]. The external surface of each membrane sample was characterized in terms of mean roughness (Ra). This parameter was obtained using different micron scan areas (4 × 4 μm²).

Characterization of produced HFs

The prepared HFs were characterized according to the procedures described in great details in our earlier works [26, 29-31]. The effective surface porosity (ϵ/L_p) and the mean pore radius ($r_{p,m}$) of the HFs were determined by gas permeation experiment using helium gas. The details of the gas permeation test and the method to obtain for this effective porosity, ϵ/L_p , and the mean pore size, $r_{p,m}$ are given elsewhere [26]. Their Contact Angle (CA) of the outer surface of the HFs was measured using the sessile drop technique [31]. The HF's wetting resistance was determined by measuring the Critical Entry water Pressure (CEPw). CEPw is the lowest pressure at the first drop of water perceived on the outer skin of HF after permeating the membrane pore from inside to outside. Determination of mechanical endurance of the HFs was carried out by measuring collapsing pressure of each HF. HF's overall porosity (ϵ_m) was obtained by the gravimetric method [29]. Scanning Electron Microscopy (SEM), (tabletop microscope, TM3000), was utilized to observe the cross-sectional image of the HF. To investigate the HF's roughness (R_a) at the outer surface, the Atomic Force Microscopy (AFM) observation was performed using the AFM device (SPA 300HV, Japan). The exact details of the AFM observation are given in other work [28]. The SEM images and the 3D AFM micrographs were presented and discussed in great details in our previous study [10].

Stripping evaluation

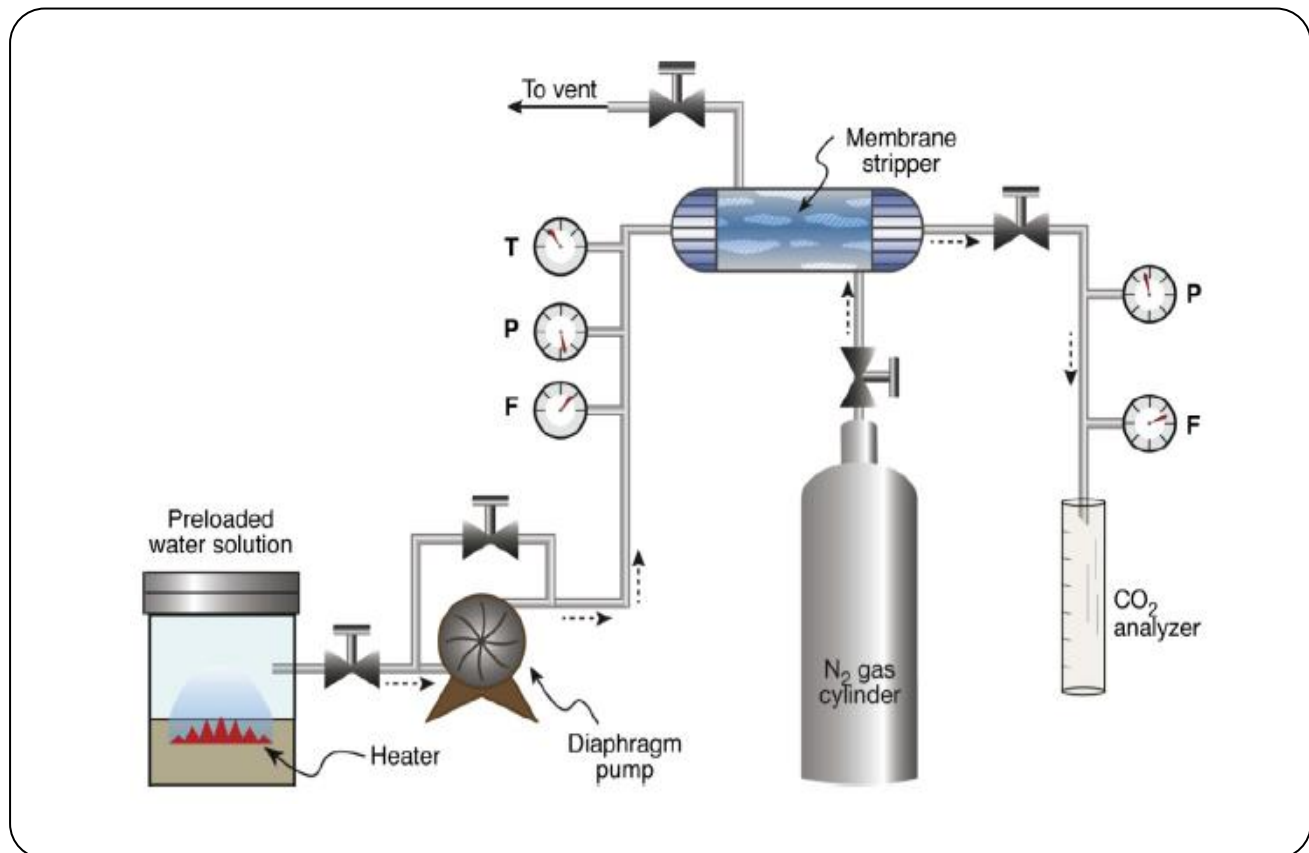
Fig. 1 shows schematically the apparatus used for CO₂ stripping by the MC system. The specifications of the stainless steel MC module used are summarized in Table 2. The aqueous DEA solution (1 DEA mol/L)

Table 1: HF Spinning conditions.

Bore flow rate (ml/min)	4.5
Bore fluid (w/w)	NMP/water (60/40)
Extrusion rate of spinning dope (ml/min)	2.00
Coagulation medium	Tap water
Spinneret dimension: o.d./i.d (mm)	1.20/0.55
Air-gap (cm)	0, 5, 10, 15, 20, 30, 50
Temperature of coagulation medium (° C)	25

Table 2: Specifications of gas-liquid MC.

Module i.d (mm)	14
Module length (mm)	270
Fiber o.d (μm)	0.7-0.9
Fiber i.d (μm)	0.45-0.5
Active length of HF (mm)	150
Number of HFs	30
Contact area (inner, mm^2)	6358.5

**Fig. 1: Schematic illustration of stripping process via MC system [33].**

or water was presaturated with pure CO₂ up to 0.0006 mol/L and loaded in the feed reservoir unless otherwise stated. The CO₂ presaturated liquid and the sweep gas (pure N₂) flowed in the lumen and shell side, respectively, in a counterflow mode. The flow rate controllers were applied to regulate the flow rates and pressures of liquid and gas streams. Dispersion of gas bubbles into the liquid was prevented by maintaining the liquid pressure 0.2×10^5 Pa higher than a gas stream. After the system reached the steady state, the CO₂ concentration in the outlet and inlet liquid was measured using the titration technique [32] and the CO₂ flux is calculated by the following Equation (1):

$$J_{\text{CO}_2} = \frac{C_{\text{l,i}} - C_{\text{l,o}}}{A_i} \times Q_l \quad (1)$$

where J_{CO_2} is the flux of CO₂ from liquid to stripping gas (mol/m²s), $C_{\text{l,i}}$ and $C_{\text{l,o}}$ are the concentration of CO₂ (mol/m³) in the liquid at the module inlet and outlet, respectively. Q_l is the liquid flowrate (m³/s) and A_i is the inner skin of the HF (m²).

RESULTS AND DISCUSSION

PVDF membranes structure

Fig. 2 represents the SEM micrographs taken of the cross-section and the external surface of the produced surface modified fibers using SMMs at the air-gaps of 0–20 cm. The HF diameters decreased from 837 to 780 μm (OD) and from 493 to 415 μm (ID) with increasing the air-gap length from 0 to 20 cm. The significant decrease in both OD and ID occurred mainly because of elongation of HF caused by gravity while travelling through the air-gap. From the figure, a porous skin layer for all membranes can be seen which is deriving from the outer and inner surfaces of the HFs and extending to the center part of HFM. Moreover, it is clear from the cross-sectional images that finger-like structure of macrovoids changed to a sponge-like structure. The size of the macrovoids in the lumen side of the HF becomes larger as the air-gap increases, which can be attributed to the longer contact time of the spun fiber with the inner coagulant. Fig. 2 (b) shows the SEM images of the external surface of the spun hollow fibers. According to the figures, the pore size decreases from 0 cm (M1) to 10 cm (M3) of the air gap and then increases from 10 cm

(M3) to 20 cm (M5). A parallel relationship is found in Table 3, according to which the pore size obtained by the gas permeation experiments shows a minimum at M3. This is also reflected in the data on overall porosity which has shown a minimum at M3.

AFM observation

The 3D AFM micrographs of the external surface of the HFs are shown in Fig. 3. The gradual decrease in roughness on the external surface of the produced HFs can be seen from the AFM images. According to Fig. 4, the roughness parameter decreased from 25 to 17 nm, as the length of air-the gap was changed from 0 to 20 cm. The same behavior was observed for surface modified polyethersulfone HFMs fabricated at different air-gaps when the air-gap was altered from 10 to 50 cm and it was ascribed to more presence of SMM at the surface of HFM. It is also interesting to note that polymer nodules are better aligned to the spinning direction with increasing the air-gap. The nodule alignment in the internal and external surfaces of the HF has also been found by other researchers [34, 35].

Characteristics of hollow fiber membranes

The experimental results obtained from the various characterization tests are summarized in Table 3. It can be seen that the mean membrane pore radius decreased with increasing air-gap up to 10 cm and then started to increase sharply from 10 to 20 cm. The large value of mean pore size at the air-gap of 20 cm, validates more presence of SMM corresponding to the large air-gap and its ability to enlarge pores. The porosity exhibited a trend opposite to the mean pore radius. The CA increased as the air gap increased up to 10 cm, indicating the gradual migration of hydrophobic SMM to the outer surface, and then leveled off. CEPw also showed a maximum at 10 cm air-gap. Thus, the air-gap of 10 cm is considered as a critical value both in terms of mean pore size and CEPw. Surprisingly, however, CEPw decreased only a little despite an order of magnitude increase in the mean pore size. This is probably due to the increase in surface hydrophobicity from air-gap of 10 cm to 20 cm caused by the continuing surface migration of SMM, which is not necessarily reflected in CA because of CA is also affected by the pore size. The AFM showed a gradual decline in the roughness of the outer surface with

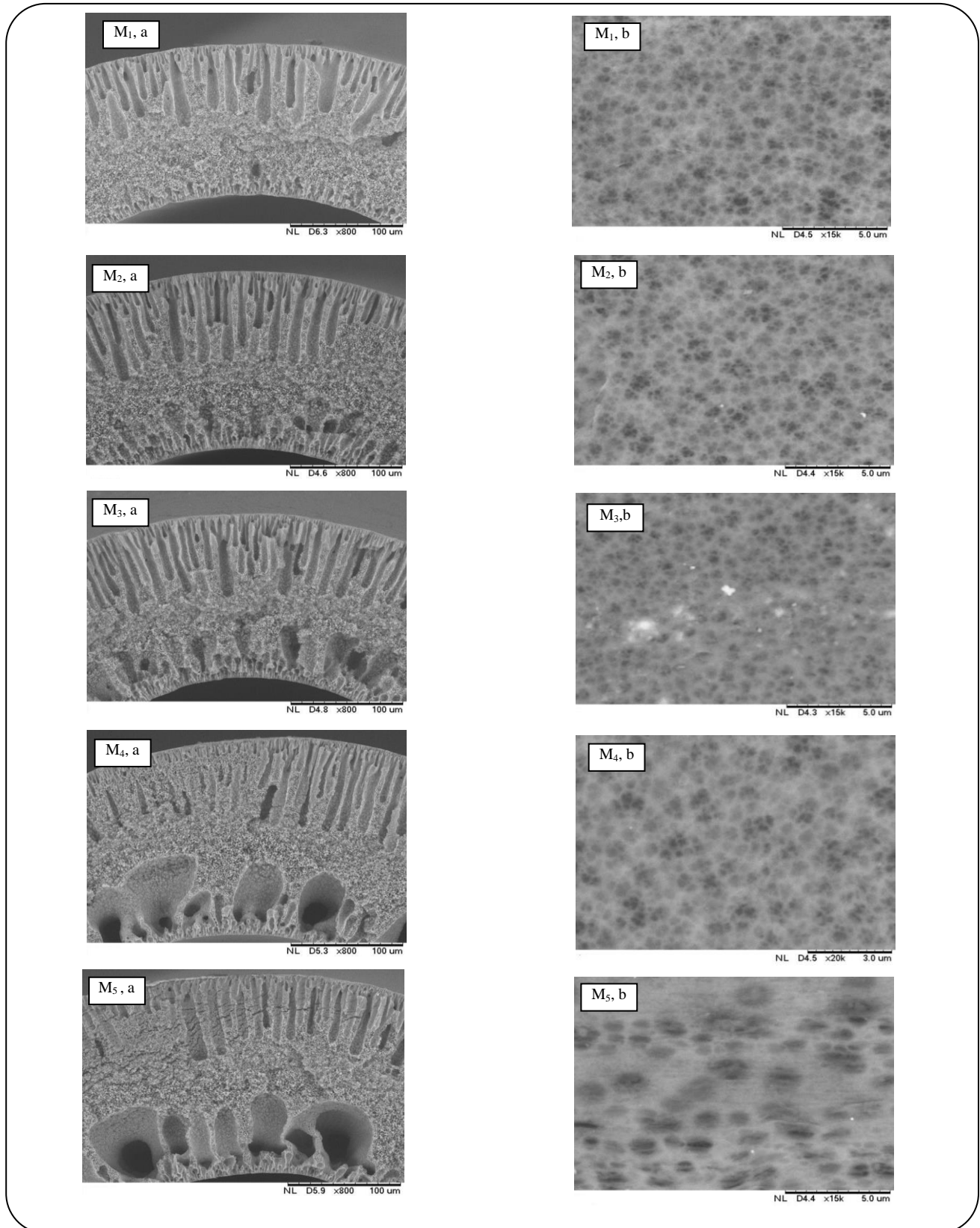


Fig. 2: SEM micrographs of surface modified PVDF membranes spun at different air-gaps (a), cross-section, (b) outer surface.

Table 3: Characterization results of PVDF membranes.

Membrane number	Air-gap distance (cm)	Average pore size (nm)	Effective surface porosity ($\frac{m^2}{g}$)	CEPw (outer surface, $\times 10^5$ Pa)	Contact angle (outer surface, °)	Collapsing pressure ($\times 10^5$ Pa)	Overall porosity (%)	Roughness ($R_{a, nm}$)
M ₁	0	36.21	118.29	3	95.09±1.30	6.5	80±1.23	24.3
M ₂	5	27.15	352.70	3.5	98.82±0.82	7	77±0.87	23.82
M ₃	10	13.57	467.42	5	101.28±0.96	7	76±1.76	21.2
M ₄	15	54.32	26.78	4.5	102.26±1.86	7.5	76±0.89	18.5
M ₅	20	301.7	10.83	4	101.95±1.34	8	75±1.54	16.35

increasing the air-gap, which could also be attributed to the presence of a larger amount of SMM at the outer skin of HF's [36].

Results of CO₂ stripping experiment

Fig. 4 shows the relationship between liquid (1 mol/L, DEA) velocity and the stripping flux at 80 °C for the PVDF membranes. The figure demonstrates a trend of increase in stripping flux with increasing DEA velocity, which according to *Simioni et al.* [12] can be ascribed to the decreased liquid flow boundary layer resistance. The stripping flux showed a maximum of 3.34×10^{-2} (mol/m² s) at liquid velocity (DEA) of 0.7 (m/s). Fig. 5 shows a similar data when the liquid is water. It should be noted that the stripping evaluation for both DEA solution and water was conducted at the same operational conditions and modes. In Tables 4 and 5 comparisons are made between CO₂ stripping flux from the aqueous DEA solution and water, respectively, through the PVDF HFMs fabricated in this work and those reported in the literature [1, 26, 37]. In both Tables, M₃, fabricated in this work with the air-gap of 10 cm, shows the highest stripping flux.

The influence of gas velocity on stripping flux is illustrated in Fig. 46 for both DEA solution and water. The data for M₃ HF (10 cm air-gap) presented but all other membranes would show a similar trend. As Fig. 6 indicates, no significant CO₂ desorption flux was observed as the gas velocity was increased from 0.005 to 0.02 (m/s). This result is in agreement with the interpretations by *Khaisri et al.* [3] that the mass transfer

rate of MC stripping is governed primarily by the liquid stream and the gas side mass transfer resistance exerts negligible influence on stripping flux.

Temperature effect on the stripping performance of M₃ HF, was also conducted and the results presented for water and DEA solution in Figs. 7 and 8, respectively. We can see from Fig. 7 that there is marked enhancement of stripping flux from 6.5×10^{-5} to 1.34×10^{-3} (mol/m² s) as the water temperature is varied from 25 to 80 °C, which can be well correlated to the decline of CO₂ solubility as the water temperature rises [6]. Also, Fig. 8 reveals that stripping flux of CO₂ is enhanced with increasing DEA temperature. According to *Khaisri et al.* [3], the temperature exerts a direct influence on the diffusion coefficient, the equilibrium constant of a chemical reaction and equilibrium partial pressure of CO₂. A reduction in the equilibrium constant of the reaction (Eq. (2)) results in an increase of CO₂ partial pressure in the gas phase by the factors of 5 to 8 corresponding to the temperature increase of 10 °C [38]. As a consequence, it can be said that the increase of the operating temperature results in elevation of the driving force for CO₂ stripping from the DEA solution.

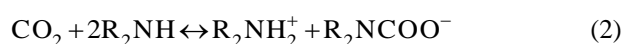


Fig. 9 demonstrates the influence of DEA concentration on stripping flux in the MC. As it can be seen from the figure increase of DEA concentration from 0.25 to 1M caused the enhancement of stripping flux, which can be confirmed by the reaction given by Eq. (2) [39]. According to *Rahbari-Sisakht et al.* [26], the rise

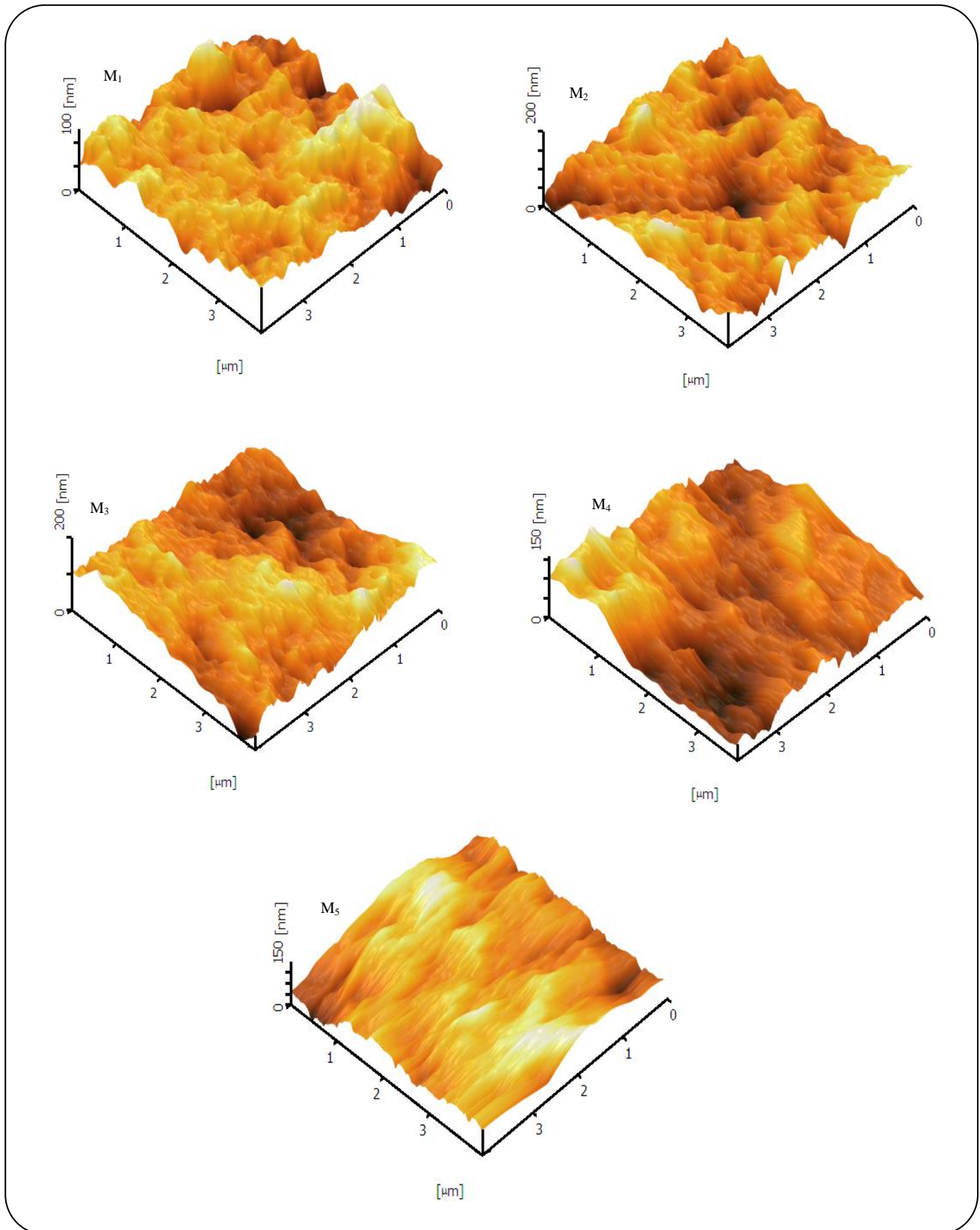


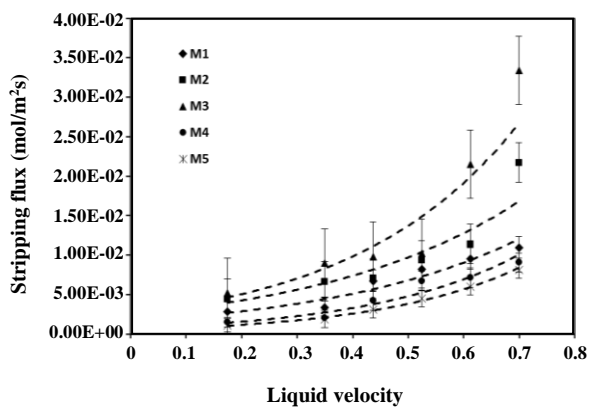
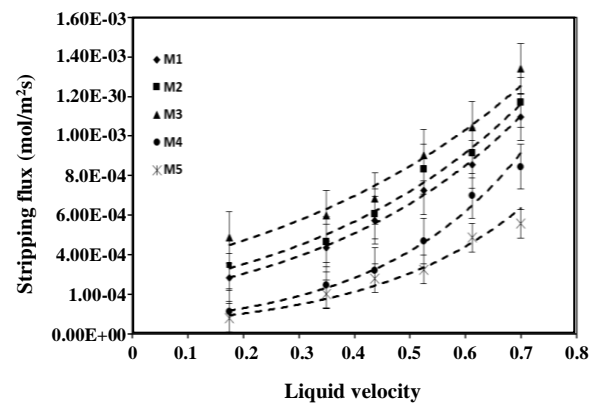
Fig. 3: 3D AFM micrographs of the outer surface of HFs.

Table 4: Results of CO₂ stripping flux from DEA solution for different PVDF fibers.

PVDF Membrane	Air-gap (cm)	Additive	CO ₂ flux (mol/m ² s)	Reference	Liquid Absorbent
M ₁	0	1wt% SMM	1.10×10 ⁻²	This work	DEA
M ₂	5	1wt% SMM	2.17×10 ⁻²	This work	DEA
M ₃	10	1wt% SMM	3.34×10 ⁻²	This work	DEA
M ₄	15	1wt% SMM	9.05×10 ⁻³	This work	DEA
M ₅	20	1wt% SMM	8.10×10 ⁻³	This work	DEA
-	0	-	2.00×10 ⁻²	[1]	DEA
-	0	5wt% PEG	3.20×10 ⁻²	[1]	DEA
-	5	1wt% SMM	1.20×10 ⁻³	[26]	DEA

Table 5: Results of CO₂ stripping from water for different PVDF HF's.

PVDF Membrane	Air-gap (cm)	Additive	CO ₂ flux (mol/m ² s)	Reference	Liquid Absorbent
M ₁	0	1wt% SMM	1.10×10 ⁻³	This work	water
M ₂	5	1wt% SMM	1.17×10 ⁻³	This work	water
M ₃	10	1wt% SMM	1.34×10 ⁻³	This work	water
M ₄	15	1wt% SMM	0.84×10 ⁻³	This work	water
M ₅	20	1wt% SMM	0.56×10 ⁻³	This work	water
-	0.5	glycerol	3.00×10 ⁻⁹	[37]	water

**Fig. 4: CO₂ stripping flux vs. liquid velocity (DEA solution).** ($T_{DEA}=80\text{ }^{\circ}\text{C}$, $M_{DEA}=1\text{ mol/L}$, gas flow rate = 50 ml/min).**Fig. 5: CO₂ stripping flux vs. liquid velocity (water).** ($T=80\text{ }^{\circ}\text{C}$, gas flow rate = 50 ml/min).

in DEA concentration leads to an increase of absorbed CO₂ during preloading in the form of R₂NCOO⁻ ion. During the stripping process, the release of CO₂ elevates the CO₂ partial pressure at the interface, resulting in enhancement of driving force [3].

CONCLUSIONS

The SMM blended PVDF hollow fiber membranes were spun at different air-gaps (0 to 20cm) in this work and used for CO₂ stripping by gas-liquid membrane contactor from aqueous DEA solution and water.

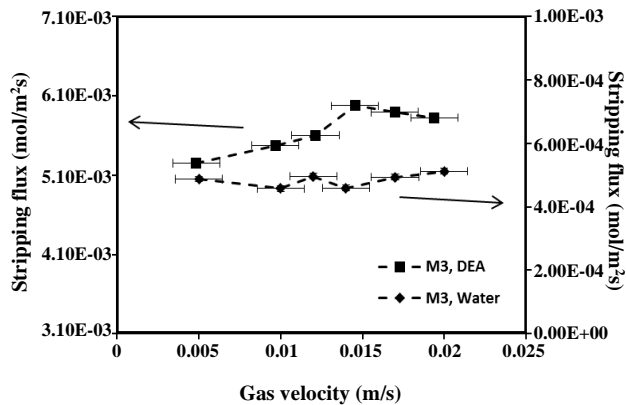


Fig. 6: CO_2 stripping flux vs. gas velocity. ($T_{\text{DEA \& Water}} = 80^\circ\text{C}$, $M_{\text{DEA}} = 1 \text{ mol/L}$, liquid flow rate = 50 ml/min).

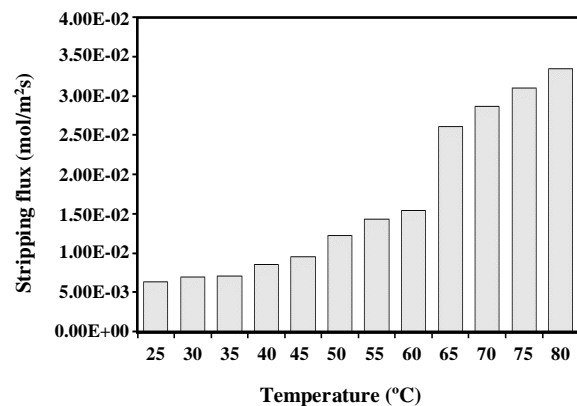


Fig. 8: CO_2 stripping flux vs. liquid phase temperature (DEA) (liquid and gas flow rate = 200, 50 ml/min, respectively).

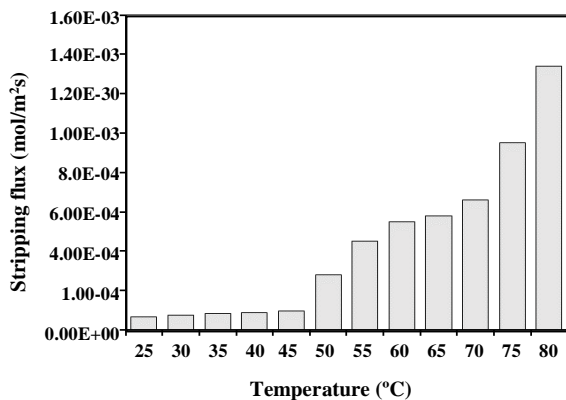


Fig. 7: CO_2 stripping flux vs. liquid phase temperature (water) (liquid and gas flow rate = 200, 50 ml/min, respectively).

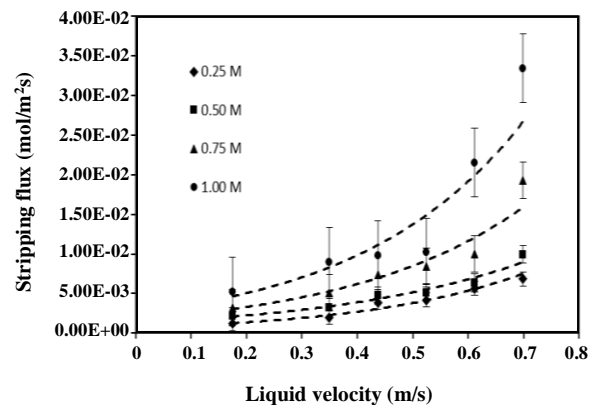


Fig. 9: CO_2 stripping flux vs. liquid velocity for various DEA concentration (gas flow rate = 50 ml/min, $T = 80^\circ\text{C}$).

The fabricated membranes were characterized in terms of contact angle and critical water entry pressure measurement to evaluate the hollow fibers hydrophobicity and wetting resistance, respectively. The pure helium permeation experiments were also conducted to obtain membrane pore size and effective porosity. Morphology of the HFs was investigated by scanning electron microscopy and atomic force microscopy. The SEM images showed that both outer and inner diameters of hollow fibers decreased significantly by increasing the air-gap length which mainly because of elongation of hollow fiber caused by gravity while travelling through the air-gap. Also, the gradual decrease in roughness on the external surface of the produced hollow fibers was observed from the AFM images. From CO_2 stripping experiment, it was found that the increase of liquid phase velocity enhances the CO_2 stripping flux. By using

hollow fiber membrane which fabricated under 10 cm air-gap the maximum stripping flux of 3.34×10^{-2} and 6.83×10^{-4} ($\text{mol/m}^2 \text{ s}$) was achieved for DEA solution and water, respectively. The gas flow velocity exhibited no significant effect on CO_2 stripping flux. Besides, it was found that the increase of temperature from 25 to 80°C led to the marked enhancement of stripping flux from 6.30×10^{-3} to 3.34×10^{-2} ($\text{mol/m}^2 \text{ s}$) and 6.5×10^{-5} to 1.34×10^{-3} ($\text{mol/m}^2 \text{ s}$), for DEA solution and water, respectively. Furthermore, the increase in DEA concentration from 0.25 to 1 mol/L, led to the enhancement of the stripping flux from 6.84×10^{-3} to 3.34×10^{-2} ($\text{mol/m}^2 \text{ s}$) at a liquid velocity of 0.7 m/s. It can be concluded from the experimental results that the data obtained from the hollow fiber spun at the optimum air-gap distance (10 cm) surpasses the stripping performance data reported in the literature.

Nomenclature

ε/L_p	Effective surface porosity, m ⁻¹
$r_{p,m}$	Mean pore size, nm
ε_m	HF's overall porosity
J_{CO_2}	CO ₂ stripping flux, mol/m ² .s
Q_l	Liquid flowrate, m ³ /s
$C_{l,i}$	CO ₂ concentration in the liquid at the module inlet, mol/m ³
$C_{l,o}$	CO ₂ concentration in the liquid at the module outlet, mol/m ³
A_i	Inner surface of the HF, m ²

Subscripts

l	Liquid
i	Inlet
o	Outlet

Greek letters

ε	Porosity
---------------	----------

Received: May 2, 2016; Accepted: Oct. 16, 2017

REFERENCES

- [1] Naim R., Ismail A.F., Cheer N.B., Abdullah M.S., Polyvinylidene Fluoride and Polyetherimide Hollow Fiber Membranes for CO₂ Stripping in Membrane Contactor, *Chemical Engineering Research and Design*, **92**(7): 1391-1398 (2014).
- [2] Koonaphapdeelert S., Wu Z., Li K., Carbon Dioxide Stripping in Ceramic Hollow Fibre Membrane Contactors, *Chemical Engineering Science*, **64**(1): 1-8 (2009).
- [3] Khaisri S., deMontigny D., Tontiwachwuthikul P., Jiraratananon R., CO₂ Stripping from Monoethanolamine Using a Membrane Contactor, *Journal of Membrane Science*, **376**(1-2): 110-118 (2011).
- [4] Rahbari-Sisakht M., Ismail A.F., Rana D., Matsuura T., Effect of Novel Surface Modifying Macromolecules on Morphology and Performance of Polysulfone Hollow fiber Membrane Contactor for CO₂ Absorption, *Separation and Purification Technology*, **99**: 61-68 (2012).
- [5] Rahbari-Sisakht M., Ismail A.F., Rana D., Matsuura T., Emadzadeh D., Effect of SMM Concentration on Morphology and Performance of Surface Modified PVDF Hollow Fiber Membrane Contactor for CO₂ Absorption, *Separation and Purification Technology*, **116**: 67-72 (2013).
- [6] Rahbari-Sisakht M., Ismail A.F., Rana D., Matsuura T., Emadzadeh D., Carbon Dioxide Stripping from Water Through Porous Polysulfone Hollow Fiber Membrane Contactor, *Separation and Purification Technology*, **108**: 119-123 (2013).
- [7] Ghasem N., Al-Marzouqi M., Duaidar A., Effect of Quenching Temperature on the Performance of Poly(vinylidene fluoride) Microporous Hollow Fiber Membranes Fabricated via Thermally Induced Phase Separation Technique on the Removal of CO₂ from CO₂-Gas Mixture, *International Journal of Greenhouse Gas Control*, **5**(6): 1550-1558 (2011).
- [8] Ghasem N., Al-Marzouqi M., Duidar A., Effect of PVDF Concentration on the Morphology and Performance of Hollow Fiber Membrane Employed as Gas-Liquid Membrane Contactor for CO₂ Absorption, *Separation and Purification Technology*, **98**: 174-185 (2012).
- [9] Ghasem N., Al-Marzouqi M., Abdul Rahim N., Modeling of CO₂ Absorption in a Membrane Contactor Considering Solvent Evaporation, *Separation and Purification Technology*, **110**: 1-10 (2013).
- [10] Korminouri F., Rahbari-Sisakht M., Rana D., Matsuura T., Ismail A.F., Study on the Effect of Air-Gap Length on Properties and Performance of Surface Modified PVDF Hollow Fiber Membrane Contactor for Carbon Dioxide Absorption, *Separation and Purification Technology*, **132**: 601-609 (2014).
- [11] Korminouri F., Rahbari-Sisakht M., Matsuura T., Ismail A.F., Surface Modification of Polysulfone Hollow Fiber Membrane Spun under Different air-Gap Lengths for Carbon Dioxide Absorption in Membrane Contactor System, *Chemical Engineering Journal*, **264**: 453-461 (2015).
- [12] Simioni M., Kentish S.E., Stevens G.W., Membrane Stripping: Desorption of Carbon Dioxide from Alkali Solvents, *Journal of Membrane Science*, **378**(1-2): 18-27 (2011).
- [13] Rahbari-Sisakht M., Korminouri F., Emadzadeh D., Matsuura T., Ismail A.F., Effect of Air-Gap Length on Carbon Dioxide Stripping Performance of a Surface Modified Polysulfone Hollow Fiber Membrane Contactor, *RSC Advances*, **4**(103): 59519-59527 (2014).

- [15] Suk D.E., Matsuura T., Park H.B., Lee Y.M., Synthesis of a New Type of Surface Modifying Macromolecules (nSMM) and Characterization and Testing of nSMM Blended Membranes for Membrane Distillation, *Journal of Membrane Science*, **277**(1–2): 177-185 (2006).
- [16] Tsai H.A., Huang D.H., Fan S.C., Wang Y.C., Li C.L., Lee K.R., Lai J.Y., Investigation of Surfactant Addition Effect on the Vapor Permeation of Aqueous Ethanol Mixtures Through Polysulfone Hollow Fiber Membranes, *Journal of Membrane Science*, **198**(2): 245-258 (2002).
- [17] Zhang X., Wen Y., Yang Y., Liu L., Effect of Air-Gap Distance on the Formation and Characterization of Hollow Polyacrylonitrile (PAN) Nascent Fibers. *Journal of Macromolecular Science, Part B.*, **47**(6): 1039-1049 (2008).
- [18] Liu R.X., Qiao X.Y., Chung T.-S., Dual-Layer P84/Polyethersulfone Hollow Fibers for Pervaporation Dehydration of Isopropanol, *Journal of Membrane Science*, **294**(1–2): 103-114 (2007).
- [19] Khulbe K.C., Feng C.Y., Hamad F., Matsuura T., Khayet M., Structural and Performance Study of Micro Porous Polyetherimide Hollow Fiber Membranes Prepared at Different Air-Gap, *Journal of Membrane Science*, **245**(1–2): 191-198 (2004).
- [20] Wang D., Li K., Teo W.K., Highly Permeable Polyethersulfone Hollow Fiber Gas Separation Membranes Prepared Using Water as Non-Solvent Additive, *Journal of Membrane Science*, **176**(2): 147-158 (2000).
- [21] Khayet M., The Effects of Air Gap Length on the Internal and External Morphology of Hollow Fiber Membranes, *Chemical Engineering Science*, **58**(14): 3091-3104 (2003).
- [22] Khayet M., García-Payo M.C., Qusay F.A., Zubaidy M.A., Structural and Performance Studies of Poly(vinyl chloride) Hollow Fiber Membranes Prepared at Different Air Gap Lengths, *Journal of Membrane Science*, **330**(1–2): 30-39 (2009).
- [23] Naim R., Ismail A.F., Mansourizadeh A., Effect of Non-Solvent Additives on the Structure and Performance of PVDF Hollow Fiber Membrane Contactor for CO₂ Stripping, *Journal of Membrane Science*, **423–424**: 503-513 (2012).
- [24] Naim R., Khulbe K.C., Ismail A.F., Matsuura T., Characterization of PVDF Hollow Fiber Membrane for CO₂ Stripping by Atomic Force Microscopy Analysis, *Separation and Purification Technology*, **109**: 98-106 (2013).
- [25] Mansourizadeh A. Ismail A.F., Influence of Membrane Morphology on Characteristics of Porous Hydrophobic PVDF Hollow Fiber Contactors for CO₂ Stripping from Water, *Desalination*, **287**: 220-227 (2012).
- [26] Rahbari-Sisakht M., Ismail A.F., Rana D., Matsuura T., Carbon Dioxide Stripping from Diethanolamine Solution Through Porous Surface Modified PVDF Hollow Fiber Membrane Contactor, *Journal of Membrane Science*, **427**: 270-275 (2013).
- [27] Ismail A.F., Dunkin I.R., Gallivan S.L., Shilton S.J., Production of Super Selective Polysulfone Hollow Fiber Membranes for Gas Separation, *Polymer*, **40**(23): 6499-6506 (1999).
- [28] Rahbari-Sisakht M., Ismail A.F., Matsuura T., Development of Asymmetric Polysulfone Hollow Fiber Membrane Contactor for CO₂ Absorption, *Separation and Purification Technology*, **86**: 215-220 (2012).
- [29] Rahbari-sisakht M., Ismail A.F., Matsuura T., Effect of Bore Fluid Composition on Structure and Performance of Asymmetric Polysulfone Hollow Fiber Membrane Contactor for CO₂ Absorption, *Separation and Purification Technology*, **88**: 99-106 (2012).
- [30] Rahbari-Sisakht M., Ismail A.F., Rana D., Matsuura T., A Novel Surface Modified Polyvinylidene Fluoride Hollow Fiber Membrane contactor for CO₂ Absorption, *Journal of Membrane Science*, **415–416**: 221-228 (2012).
- [31] Khayet M., Feng C.Y., Khulbe K.C., Matsuura T., Study on the Effect of a Non-Solvent Additive on the Morphology and Performance of Ultrafiltration Hollow-Fiber Membranes, *Desalination*, **148**(1–3): 321-327 (2002).
- [32] Li M.-H. Chang B.-C., Solubilities of Carbon Dioxide in Water + Monoethanolamine + 2-Amino-2-methyl-1-propanol. *Journal of Chemical & Engineering Data*. **39**(3): 448-452 (1994).

- [33] Rahbari-Sisakht M., Rana D., Matsuura T., Emadzadeh D., Padaki M., Ismail A.F., [Study on CO₂ Stripping from Water Through Novel Surface Modified PVDF Hollow Fiber Membrane Contactor](#), *Chemical Engineering Journal*, **246**: 306-310 (2014).
- [34] Khulbe K.C., Feng C.Y., Matsuura T., Mosqueada-Jimenez D.C., Rafat M., Kingston D., Narbaitz R.M., Khayet M., [Characterization of Surface-Modified Hollow Fiber Polyethersulfone Membranes Prepared at Different Air Gaps](#), *Journal of Applied Polymer Science*, **104**(2): 710-721 (2007).
- [35] Mansourizadeh A. Ismail A.F., [CO₂ Stripping from Water Through Porous PVDF Hollow Fiber Membrane Contactor](#), *Desalination*, **273**(2-3): 386-390 (2011).
- [36] Weiland R.H., Rawal M., and Rice R.G., [Stripping of Carbon Dioxide from Monoethanolamine Solutions in a Packed Column](#), *AIChE Journal*, **28**(6): 963-973 (1982).
- [37] Mokhatab S., Poe W.A., Speight J.G., ["Handbook of Natural Gas Transmission and Processing"](#), Gulf Professional Publishing, Burlington (2006).